

Distribution Agreement

In presenting this thesis as a partial fulfillment of the requirements for a degree from Emory University, I hereby grant to Emory University and its agents the non-exclusive license to archive, make accessible, and display my thesis in whole or in part in all forms of media, now or hereafter now, including display on the World Wide Web. I understand that I may select some access restrictions as part of the online submission of this thesis. I retain all ownership rights to the copyright of the thesis. I also retain the right to use in future works (such as articles or books) all or part of this thesis.

John Claiborne Owens

16 April 2013

Designing a Magnetometer

by

John Claiborne Owens

Dr. Sergei Urazhdin
Adviser

Department of Physics

Dr. Sergei Urazhdin
Adviser

Dr. Vincent Huynh
Committee Member

Dr. Jed Brody
Committee Member

Dr. Jose Soria
Committee Member

2013

Designing a Magnetometer

By

Clai Owens

Dr. Sergei Urazhdin

Adviser

An abstract of
a thesis submitted to the Faculty of Emory College of Arts and Sciences
of Emory University in partial fulfillment
of the requirements of the degree of
Bachelor of Sciences with Honors

Department of Physics

2013

Abstract

Designing a Magnetometer

By John Claiborne Owens

We have previously investigated magnetic properties of platinum thin films. In order to continue measurements on the magnetic properties of platinum, we needed an instrument to measure the magnetization of thin films. This paper discusses our design and construction of a vibrating sample magnetometer (VSM). This device measures the magnetic moment of a sample by vibrating the sample between pick-up coils. The induced EMF in the coils is proportional to the magnetic moment of the sample. We control the frequency and amplitude of vibrations by using a modified speaker as a vibrator connected to a source of oscillating voltage. At first, we induced magnetization in our samples by using electromagnets to generate an external field, and the VSM we built was able to measure magnetization of large samples. The current that powers the electromagnets produced too much magnetic noise, so we are redesigning the VSM using permanent magnets instead. This design achieves much lower noise. Future work will include finishing the final design of the magnetometer and making measurements of the magnetization of thin film ferromagnets.

Designing a Magnetometer

By

John Claiborne Owens

Dr. Sergei Urazhdin

Adviser

A thesis submitted to the Faculty of Emory College of Arts and Sciences
of Emory University in partial fulfillment
of the requirements of the degree of
Bachelor of Sciences with Honors

Department of Physics

2013

Contents

I	Introduction	1
1	Magnetization	1
2	Methods of Measuring Magnetization	3
3	The Vibrating Sample Magnetometer	4
4	My Project	5
4.1	Background and Motivation	5
4.2	Designing a VSM	7
II	Methodology and Results	12
5	Powering the Speaker	12
6	Mechanical Assembly	14
7	Pick-up Coils	16
8	Testing the Magnetometer	18
9	New Design	23
III	Conclusion and Future Work	25

List of Figures

1	The field required to switch the direction of magnetization of the free ferromagnetic layer at different temperatures and thicknesses of the platinum layer. From reference 1.	6
2	Basic schematic of a VSM	8
3	Diagram of our coil orientation. The black arrows on the coils indicate the direction the coils are wired.	10
4	A picture of the completed speaker amplifier. The large black object is the heat sink we added.	13
5	A top-down view of the magnets we intended to use to induce magnetization in the samples. We want the sample to be in between the magnetic poles. Our coils will be in a frame that clamps to the poles of the magnet.	15
6	The speaker, the speaker support, and the carbon fiber rod.	16
7	The pick-up coils inside the frame that attaches them to the external magnet. First, the large central hole fits around the magnetic pole. Then, a screw tightens the clamp around the magnetic pole.	17
8	Voltage amplitude at the reference frequency (This will be the signal when the sample is present) and noise as a function of frequency when the lock-in amplifier is disconnected from the coils.	19
9	Noise as a function of frequency when no sample is attached and the external magnet is off. The amplitude is constant at 0.05 volts.	20
10	Plots of the noise when the magnet is set to 1000 Oe, 0 Oe, and when the magnet is turned off.	21

11	Here we measured the induced voltage in the coils as a function of external field.	22
12	Noise with permanent magnets used in our setup instead of the electromagnets. Note that the scale of these measurements is much smaller.	23
13	The setup for the magnetometer designed around the permanent magnets. The two magnets are on the left and right ends of the metal “t” in the center. The stepper motor is on the left.	24
14	Noise as a function of frequency for several different distances between the pick-up coils and the base of the speaker mount. Proximity to the speaker greatly increases the noise, especially as the frequency increases.	25

Part I

Introduction

1 Magnetization

Matter in an external magnetic field becomes magnetized. This is because microscopic dipoles inside the matter align in some direction [2]. This polarization is described by a vector quantity known as magnetization \vec{M} .

$$\vec{M} \equiv \text{magnetic dipole moment per unit volume} \quad (1)$$

A magnetized material creates a magnetic field dependent on the magnetization and the geometry of the sample. At large distances compared to the magnetized sample size, it produces magnetic field that can be approximated by that of a magnetic dipole. An ideal dipole is a geometry where all of the positive charge is located at one point and all of the negative charge is located at another point. The distance d between the two points approaches 0, and the charge q of each charge goes to infinity, keeping qd fixed [2]. The dipole approximation works well for our samples since the coils we use to detect the magnetic fields of our samples are much further away than the length of our samples. The field of a dipole is the following [2]:

$$\vec{B} = \frac{\mu_0}{4\pi r^3} [3(\vec{m} \cdot \hat{r})\hat{r} - \vec{m}] \quad (2)$$

where \vec{m} is the magnetic moment of the sample. Assuming the distribution of

magnetization in the sample is uniform, we can relate \vec{m} to \vec{M} by

$$\vec{m} = V\vec{M} \quad (3)$$

Materials can be characterized as paramagnets, diamagnets, or ferromagnets (other characterizations besides these exist) depending on their response to external magnetic field. Paramagnets are magnetized parallel to the external magnetic fields, diamagnets are magnetized opposite the magnetic fields, and ferromagnets retain magnetization after the external field is removed. In our experiments we work with platinum, known to be paramagnetic [3]. When an external magnetic field is applied to a paramagnet, the magnetization follows the following relationship [2]:

$$\mathbf{M} = \chi_m \mathbf{H} \quad (4)$$

where χ_m is a constant (at low fields) known as the magnetic susceptibility. However, platinum almost satisfies the Stoner criterion for ferromagnetic ordering [1, 4]. In order for ferromagnetism to occur, a material must have a high density of states near the Fermi surface and a small density of electrons. When this happens, it is more energetically favorable for electrons to be in the same spin states. Platinum almost satisfies these criteria, but the electronic states of platinum are almost completely filled to accommodate the large number of outer shell electrons. Ferromagnetism has been observed in several platinum systems, including platinum nanoparticles [5, 6, 7], nanocontacts [9, 8], nanowires [9, 10], and thin films [11, 12][11, 12].

2 Methods of Measuring Magnetization

A device that measures the magnetization of a sample is called a magnetometer. Foner [13] classifies magnetometers into three different categories. The first type of magnetometer measures magnetization by measuring the force on a sample in a non-uniform magnetic field. Wolf [14] showed some limitations of this method, especially for anisotropic crystals. Also, measuring magnetization versus applied field is difficult with this technique [13]. The second type of magnetometer measures induced voltage in detection coils moving relative to the sample [15]. Smith [16] in 1956 designed the first vibrating coil magnetometer. This technique involves vibrating detection coils around a fixed sample. The field of the sample is not uniform, so according to Faraday's law, an EMF is induced in the coils as the coils oscillate around the sample. This technique is extremely sensitive to the uniformity of the magnetic field. A vibrating sample magnetometer measures magnetization by vibrating the sample and fixing the detection coil system [15]. The VSM is simple to build but still can achieve high sensitivity. Some commercial models are able to measure magnet moments well below $1 \mu\text{emu}$ [17]. The last type of magnetometer measures magnetization indirectly by measuring phenomena associated with magnetic properties. Some examples include measurements of the Faraday effect, studying galvanomagnetic effects such as the Hall effect, and microwave ferromagnetic resonance measurements [18, 19]. These indirect magnetization measurement techniques are generally more limited, because these phenomena typically are only measurable in particular classes of materials [13].

3 The Vibrating Sample Magnetometer

The first vibrating sample magnetometer was described by Foner in 1956 [19]. In this paper he describes a VSM made in a similar fashion to how we built our VSM. He attaches one end of a drinking straw onto a speaker diaphragm, then he mounts the sample on the other end of the straw. When the speaker is turned on, it vibrates the sample at a particular amplitude and frequency. The end of the straw with the sample attached is put in between two magnetic poles in order to induce magnetization within the sample. Between the poles and the sample he puts pick-up coils to measure the change in magnetic flux caused by the moving sample. Since Foner's design, numerous papers [20, 21, 22, 23, 24, 25] have been written that discuss possible improvements to the magnetometer. Each author keeps the design very similar.

More recent designs use the phase-sensitive lock-in amplifier to improve signal recovery. The lock-in amplifier is sensitive to a particular frequency and phase of voltage signals [26]. It extracts a signal with known frequency and phase from noisy measurements. The lock-in amplifier uses a low-noise, phase-adjustable reference, with the same frequency of the signal trying to be recovered. The lock-in amplifier makes use of the orthogonality of sinusoidal functions. When sinusoidal functions are multiplied by each other and integrated over a period of the wave, the integral goes to zero except when the sinusoidal functions have the same frequency. Also, the integral is maximized when the sinusoidal functions have the same phase. The lock-in amplifier adjusts the phase until the signal is at a maximum. This allows it to measure the phase of the signal compared to the reference. When the signal and the reference have the same frequency, the measured amplitude is

$$A_{measured} = \frac{A_{ref}A_{signal}}{2} \quad (5)$$

This allows the amplitude of the signal to be calculated. Thus, the lock-in amplifier can record both the amplitude of the signal, the phase of the signal relative to the reference signal, and the amplitude of the noise of the input.

4 My Project

4.1 Background and Motivation

In a previous publication, we found anomalous magnetic coupling between ferromagnets separated by a platinum layer [1]. Although platinum is typically characterized as a paramagnet, we found that a platinum spacer between two ferromagnets couples like a ferromagnet to the adjacent ferromagnetic layers. One of the ferromagnetic layer's magnetization was fixed by an adjacent antiferromagnet. The other ferromagnet layer's magnetization was free to respond to the external field and the adjacent platinum layer's magnetization. We measured the external field required to change the direction of magnetization in the free ferromagnetic layer as a function of temperature and thickness of the platinum layer. At lower temperatures larger fields were required to switch the direction of magnetization of the free ferromagnetic layer. As the thickness of the platinum layer increased, less field was required to switch the direction of magnetization of the free ferromagnetic layer. This can be seen from our data:

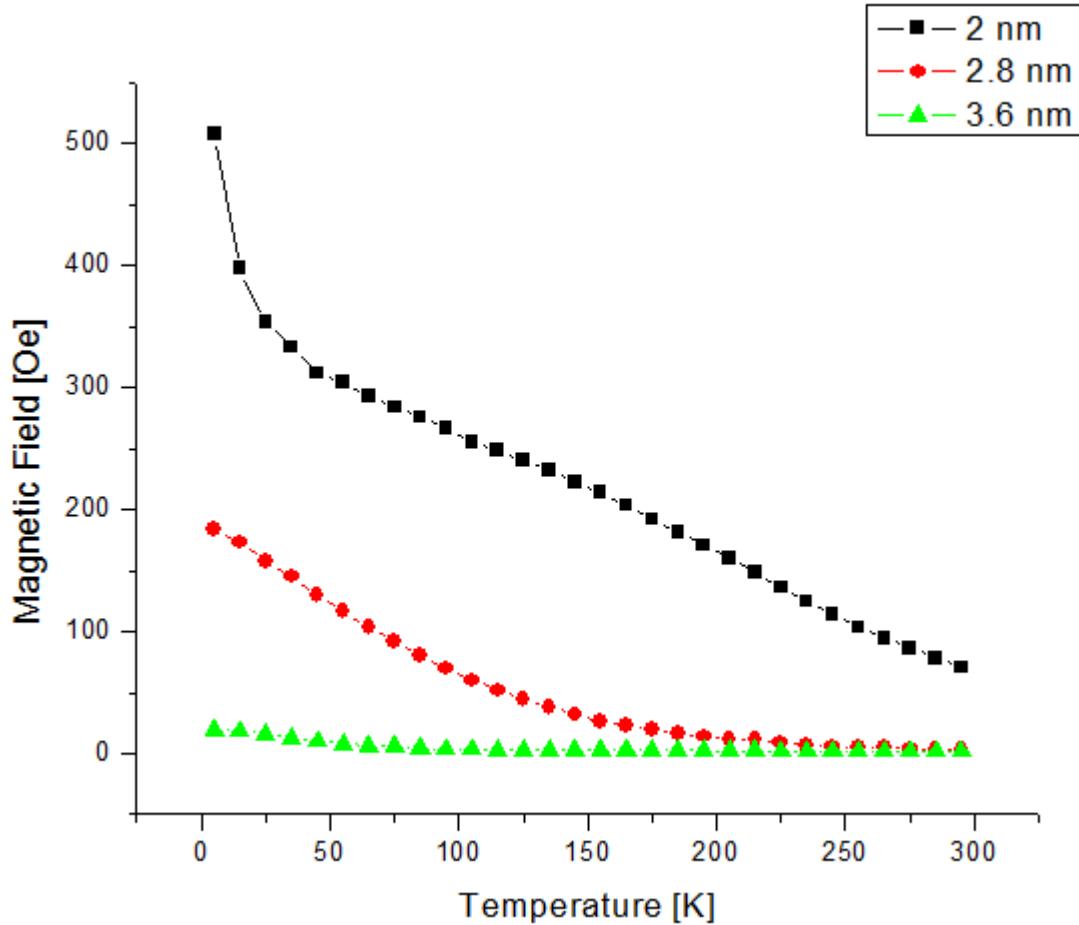


Figure 1: The field required to switch the direction of magnetization of the free ferromagnetic layer at different temperatures and thicknesses of the platinum layer. From reference 1.

This dependence on temperature and thickness of the platinum layer is not explained by any previous mechanisms, such as the RKKY interaction [27, 28] or the “pinhole” interaction [29]. This anomolous behaviour led us to design a new experiment where instead of changing the thickness of the platinum layer or the temperature of the sample, we change the saturation magnetization of the ferromagnets. The ferromagnets we used were composed of permalloy, an alloy of nickel and iron. We can add different concentrations of gadolinium to the permalloy in order to change its

saturation magnetization. Different magnetizations of the ferromagnet should induce different magnetizations in platinum. Permalloy thin films made in a vacuum have saturation magnetizations on the order of 800 Oe/cm³ [30]. Estimating the volume of a thin film of thickness 3 nm to be 3×10^{-7} cm³, we estimate the magnetic moment of the film to be 2.4×10^{-4} , so we must build a device that can accurately measure magnetizations of this magnitude or lower.

With typical materials such as diamagnets and paramagnets we would expect increasing the magnetization should linearly increase the exchange field in the material, according to equation (4) [11]:

$$\mathbf{M} = \chi_m \mathbf{H}$$

Increasing the magnetization of the permalloy would increase the field required to change the direction of magnetization of the free ferromagnetic linearly if platinum were a standard diamagnet or paramagnet. From last year's measurements of the proximity magnetism in platinum[1], we expect platinum to have unique magnetic properties and have a more complicated relationship. However, we needed a method to directly measure the magnetization of the permalloy/gadolinium alloys. My project focused on building a device that could measure the magnetization of a sample.

4.2 Designing a VSM

I decided the most efficient device that I could build which measured magnetization was a vibrating sample magnetometer. The schematic of a VSM is shown below:

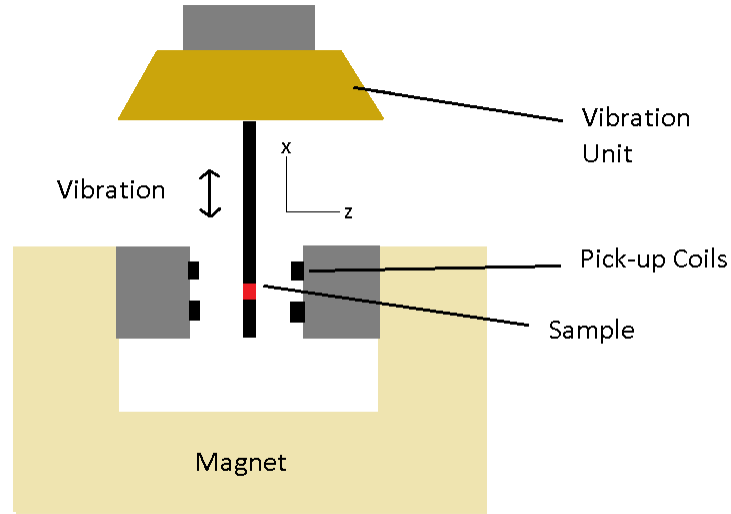


Figure 2: Basic schematic of a VSM

First, we want to estimate the magnitude of the signal we expect to measure from a sample with a magnetic moment of 2.4×10^{-4} emu. To do that, we calculate the strength of the field as function of time, distance from the sample's midpoint of vibration, and magnetization of the sample:

First we take the formula of the magnetic field for a dipole from equation (3)[11]

$$\vec{B} = \frac{\mu_0}{4\pi r^3} [3(\vec{m} \cdot \hat{r})\hat{r} - \vec{m}]$$

If we call the direction the external magnet field points \hat{z} and the direction of oscillation \hat{x} , then we can rewrite the field as

$$\vec{B} = \frac{\mu_0 m}{4\pi r^3} [3 \cos \theta \hat{r} - \hat{z}]$$

$$\vec{B} = \frac{\mu_0 m}{4\pi r^3} [3 \cos \theta (\sin \theta \cos \phi \hat{x} + \sin \theta \sin \phi \hat{y} + \cos \theta \hat{z}) - \hat{z}]$$

$$\vec{B} = \frac{\mu_0 m}{4\pi r^3} [3 \cos \theta \sin \theta \cos \phi \hat{x} + 3 \cos \theta \sin \theta \sin \phi \hat{y} + (3 \cos^2 \theta - 1) \hat{z}]$$

$$\vec{B} = \frac{\mu_0 m}{4\pi r^3} \left[3 \frac{zx}{r^2} \hat{x} + 3 \frac{zy}{r^2} \hat{y} + \left(3 \frac{z^2}{r^2} - 1 \right) \hat{z} \right] \quad (6)$$

This is the static field. If we assume that the sample undergoes small oscillations, we can model the oscillations as small changes of \vec{B} in the \hat{x} direction and use a Taylor expansion:

$$\vec{B}(x + dx, y, z) \approx \vec{B}_0 + dx \frac{\partial \vec{B}}{\partial x} \quad (7)$$

Our coils will be attached to the magnetic poles and parallel to the z direction, so the only magnetic flux that will affect the induced EMF in the coils will be the z component.

$$B_z(x + dx, y, z) = B_{z0} + dx \frac{\mu_0 m}{4\pi} \left[\frac{3x}{r^5} - \frac{15z^2 x}{r^7} \right] \quad (8)$$

\vec{B}_{0z} is constant with respect to time. Using the above relations we can estimate that:

$$\frac{\partial B_z}{\partial t} \approx v \frac{\mu_0 m}{4\pi} \left[\frac{3x}{r^5} - \frac{15z^2 x}{r^7} \right] \quad (9)$$

We input a sinusoidal voltage into the speaker that drives the oscillations of our sample. The form of v will be $X_0 \omega \sin(\omega t + \phi)$, where X_0 is the amplitude of oscillation and ω is the frequency of oscillations. The induced EMF in a detection coil can then be estimated as

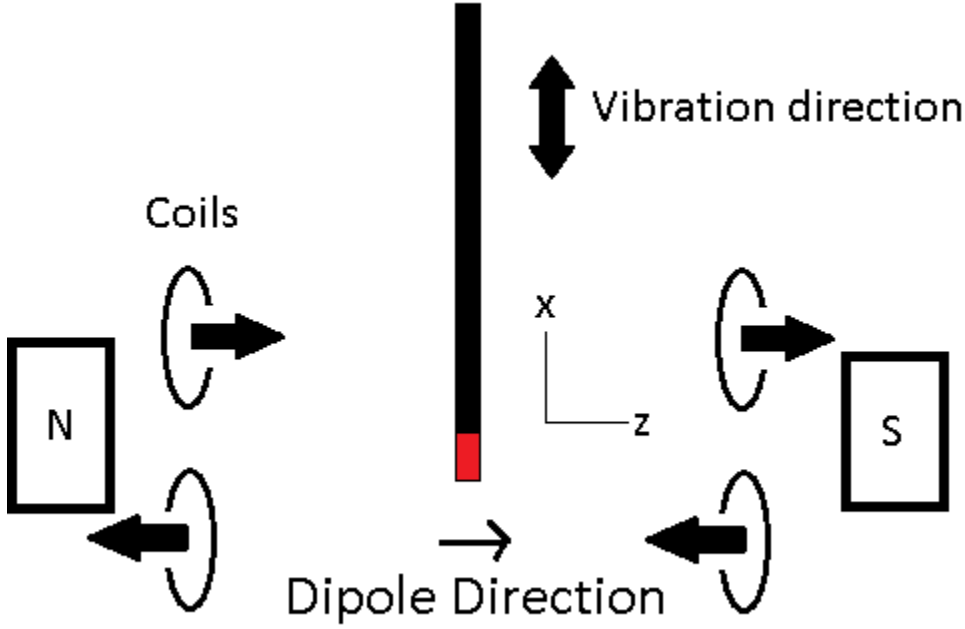


Figure 3: Diagram of our coil orientation. The black arrows on the coils indicate the direction the coils are wired.

$$\epsilon_{ind} = -N_{turns}A \frac{\partial \vec{B}_z}{\partial t} = -\frac{\mu_0 m}{4\pi} N_{turns} A X_0 \frac{3x}{r^5} \sin(\omega t + \phi) \left[1 - \frac{5z^2}{r^2} \right] \quad (10)$$

per coil, where N_{turns} is the number of turns per coil. With this formula, we learn how to optimize the position of the pick-up coils. We choose the following arrangement:

For our set-up, the easiest way to mount the coils is by clamping them to the external magnetic poles, which are on the z axis. This arrangement is known as Mallinson's configuration [key-23]. However, we deviate from this geometry slightly. Mallinson has his coil loops touching, but we put some distance between our coils not only to allow room for the coils to be clamped to the magnetic pole, but also to make the measurements less sensitive to the sample's starting position [key-25].

The benefits of this arrangement can be seen from equation (10). First, we see that equation (10) is odd with respect to x . This means that the EMF in a coil at distance x from the sample would cancel with the EMF in a coil at a distance $-x$. On the other hand, if we wire the coils in opposite directions on the x axis, the signal from the coils will add. An additional benefit will be that the EMF generated by any other external magnetic field coming from above or below the coils on the z axis will cancel because the coils are wired in opposite directions. This will reduce external noise. Equation (10) is even with respect to z , so these coils need to be wired the same direction so that the induced EMF adds. In this arrangement, EMF induced from a source in between the coils adds, but the EMF induced from a source above or below the coils will cancel.

Also, the signal is not only strongly dependent on r , but it is also dependent on the value of x and the ratio of x to z . At $x = 2z$ and $x = 0$, the signal is zero. The signal output is a maximum when $x = 0.389z$, but the EMF switches direction when $x > 2z$. Since the radius of our coils is about 1.5 cm, the ideal configuration would have $z = 1.5$ cm, so that the coils capture all of the signal from $x = 0$ to $x = \pm 2z$. Assuming this ideal arrangement, we can calculate the magnitude of our anticipated signal. We use $N_{turns} = 3000$, $X_0 = 1$ cm, $\omega = 22$ Hz, $A = 7$ cm², $x = 0.8$ cm (this is the value of x that gives the average flux through the area of the coils), $z = 1.5$ cm, and $r = 1.7$ cm and obtain a signal with a magnitude of 1.3×10^{-4} μV per $\frac{\text{emu}}{\text{cm}^3}$ of the sample. Permalloy thin film samples have a magnetization on the order of 800 $\frac{\text{emu}}{\text{cm}^3}$ [30], so the signal would be 0.1 μV .

Our first design did not take this into account, and we achieved much lower signals. We originally had the coils placed at $z = 1.5$ cm, $x = 4.0$ cm, and we measured the magnetic moment of bulk permalloy, which has a similar magnetization as permalloy in the thin films. The measured voltage would be on the order of 2.5×10^{-7} μV per

$\frac{\text{emu}}{\text{cm}^3}$ of the sample. For samples with magnetization of $750 \frac{\text{emu}}{\text{cm}^3}$ (the magnetization of bulk permalloy) [30], we anticipate signals on the order of $2 \times 10^{-4} \mu\text{V}$. The ideal coil arrangement may not be possible since we have to fit magnets in between the coils, so perhaps a coil arrangement where the coils face the \hat{x} or \hat{y} direction would be preferable.

After determining how the coils are to be arranged, we also needed to determine how to vibrate the sample effectively. We chose to use a speaker as the vibration driver. A speaker takes an AC current input and drives a diaphragm at a frequency equal to the frequency of the input current. The amplitude of oscillations is also related to the amplitude of the input current, though the relation is not necessarily linear. By gluing a rod that could hold our sample to the diaphragm of the speaker, we could build an effective sample vibrator which we could insert into our current setup for magnetic measurements. After removing systematic noise and calibrating the magnetometer using samples with known magnetizations, we would be able to measure the magnetization of our samples.

Part II

Methodology and Results

5 Powering the Speaker

Our first goal was to make the speaker respond to the oscillatory current output of our current source. We use the Signal Recovery model 7265 lock-in amplifier as our current output. The amplitude of the output oscillatory voltage can go as high as 5

volts. The speaker we used had its own amplifier built into the box in which it came. Thus, we connect the lock-in amplifier to this built-in speaker amplifier. However, a typical speaker amplifier is not made to be driven constantly for long periods of time, since a speaker is typically turned on and off frequently when making sound. For our experiments, we needed the amplifier to run for at least an hour at a time when we are taking data. In order to dissipate the large amount of heat generated by this amplifier circuit, we added a large heat sink and a fan to the amplifier (Figure 4). Also, we added a fuse and a switch, and wired output and input cables that are compatible with the lock-in amplifier and the speaker.

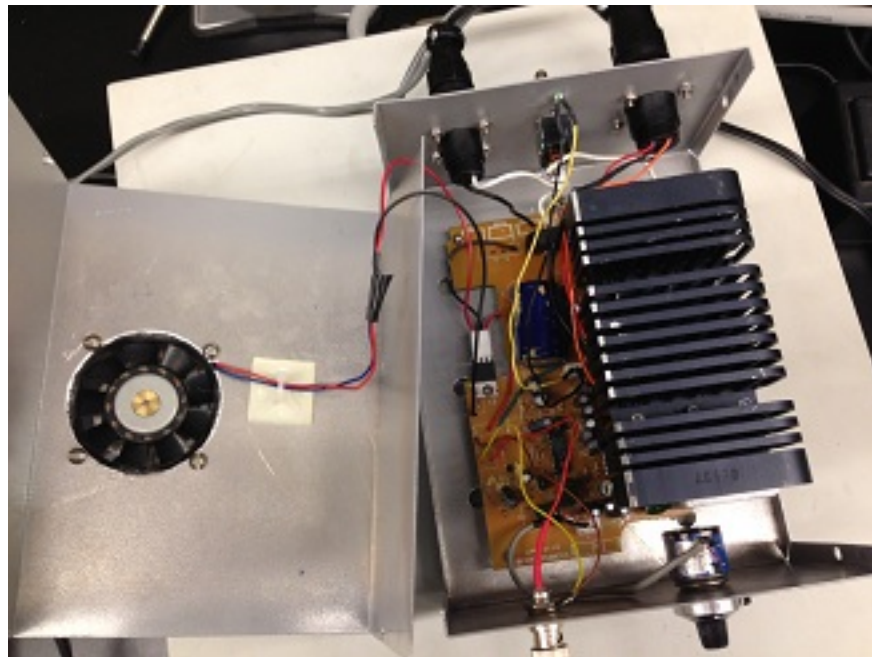


Figure 4: A picture of the completed speaker amplifier. The large black object is the heat sink we added.

After modifying the circuit by adding a voltage divider, we were able to use an oscillating voltage of 0.1 Volts on the lock-in amplifier to drive the speaker at an

amplitude of approximately 1 cm. Also, the amplifier could drive the speaker for an hour without building up significant heat. The amount the input signal was amplified depended on the frequency of the signal. Lower and higher frequencies resulted in less amplification. For signals of approximately 15 Hz, we measured an amplitude ten times higher than the original signal. For signals of 50 Hz, the output amplitude was only about 6 times as large as the input signal.

6 Mechanical Assembly

Next, we built a mechanical support system that coupled the sample to the speaker diaphragm so that the sample would be driven at the frequency and amplitude of the speaker. We also needed the sample to vibrate within the magnetic poles of the setup in Figure 6, so that we can use the magnets to induce magnetization in the samples.

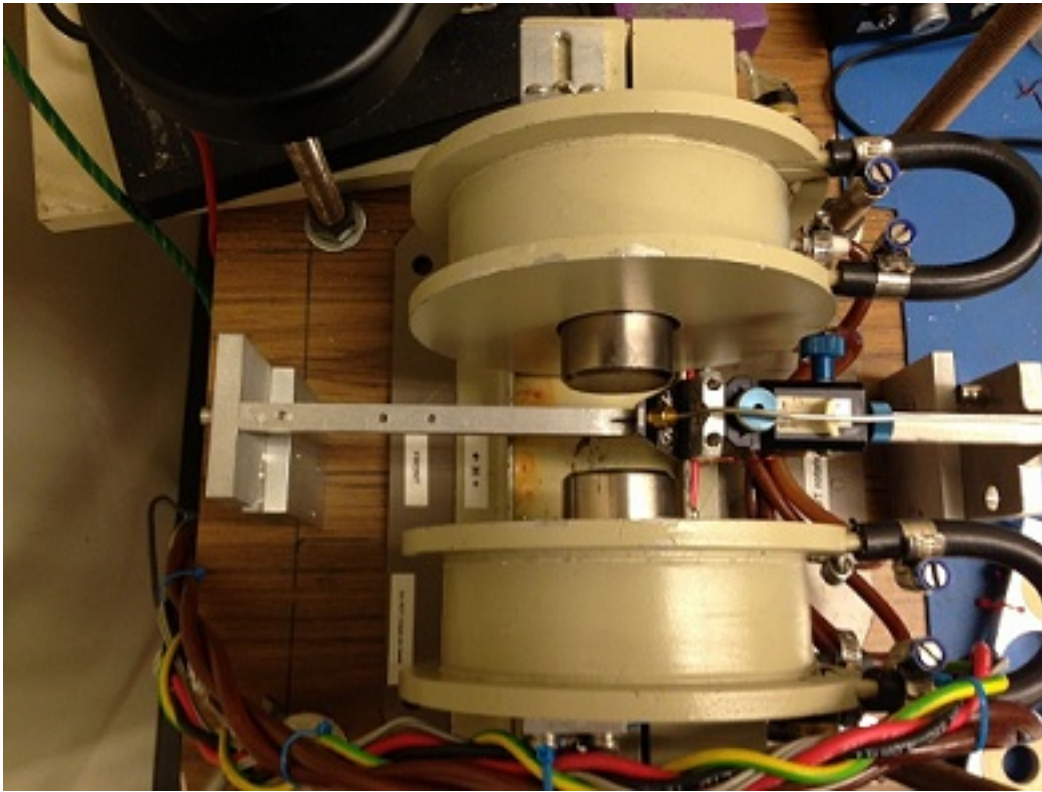


Figure 5: A top-down view of the magnets we intended to use to induce magnetization in the samples. We want the sample to be in between the magnetic poles. Our coils will be in a frame that clamps to the poles of the magnet.

A large aluminum plate (not shown) is held above the magnet in Figure 6 using thick metal poles that attach to the table on which the magnet is sitting. We built a support system for the speaker out of aluminum that fastens to the large aluminum plate. We ran a carbon fiber tube through a hole that went through the middle of the speaker, then used a clamp and a cable tie to fasten the rod to the diaphragm of the speaker. Carbon fiber is hard, but it is also light. We used linear bearings fastened on top of the speaker and at the bottom of the speaker support to ensure that the rod can only vibrate in one direction. We cut a 1 cm section of the rod halfway through at the bottom and filled the half of the tube with glue so that we have a flat surface

on which to mount our samples.

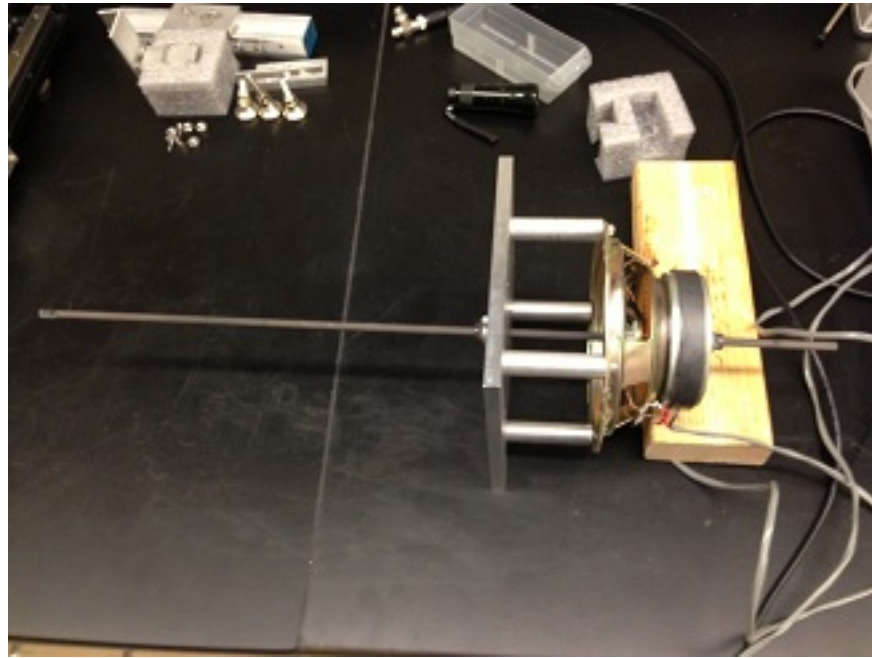


Figure 6: The speaker, the speaker support, and the carbon fiber rod.

7 Pick-up Coils

Next, we needed to build a frame in order to support the pick-up coils. We made the clamp out of aluminum not only because aluminum is easy to use but also because eddy currents in the metal outside the coils created by the vibrating sample will add to the induced signal. However, eddy currents created by our vibrating magnetic dipole would decrease the sample signal if the metal was inside the pick-up coils, so our design left no metal inside the coils. Figure 7 shows the clamps we created. The pick-up coils we used had 3000 turns. We wanted to wire the coils in such a way that induced EMF from the sample adds while the induced EMF from any external magnetic fields from other electronic equipment in the lab (including the

speaker) cancel, so we wired the coils above the sample the opposite direction of the coils below the sample. We wanted the coils on top to be facing the same way and wired the same way; however, the design of the coils made it more convenient to reverse the facing of the coils so that the coils on the same horizontal plane are facing opposite directions. In order to make these signals add, we wired the coils on the same horizontal plane in opposite directions.

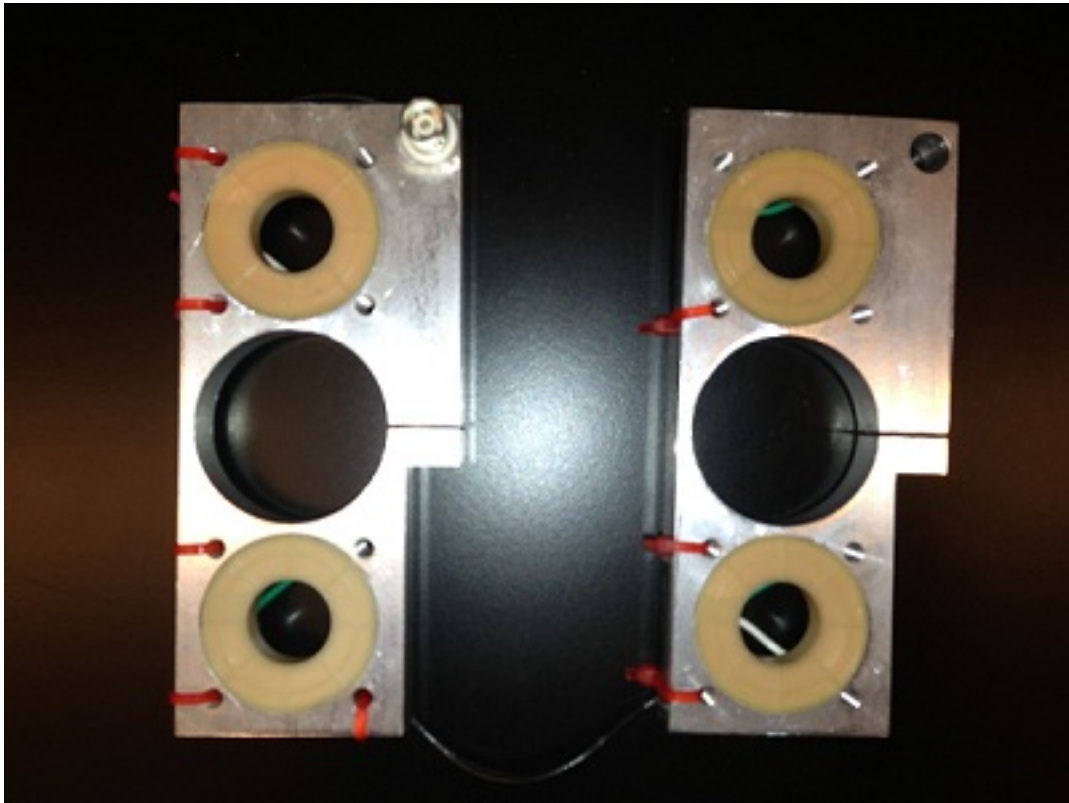


Figure 7: The pick-up coils inside the frame that attaches them to the external magnet. First, the large central hole fits around the magnetic pole. Then, a screw tightens the clamp around the magnetic pole.

After wiring all of these coils in series so that the EMFs induced by the field of the vibrating sample add, we soldered each end of the series loop to the two terminals of

a BNC adapter. We used coaxial cable in order to minimize magnetic noise induced by stray magnetic fields. The BNC adapter connected our coils to the lock-in amplifier. The lock-in amplifier not only controls the frequency of oscillations, but it also measures the signal from the coils. Since we use a sinusoidal voltage to control the speaker, the sample will oscillate sinusoidally. This means that the induced EMF in the coils will also oscillate sinusoidally (see equation (10)). The lock-in amplifier can measure the amplitude of the sine curve and the magnitude of the noise that is in our electrical measurements.

8 Testing the Magnetometer

Once we had assembled all of the parts mentioned above, we determine at what frequency and amplitude the speaker should oscillate. First, we measured the noise and signal as a function of frequency when the pick up coils were not actually hooked to the lock-in amplifier, so that we can see the noise just generated by the lock-in amplifier.

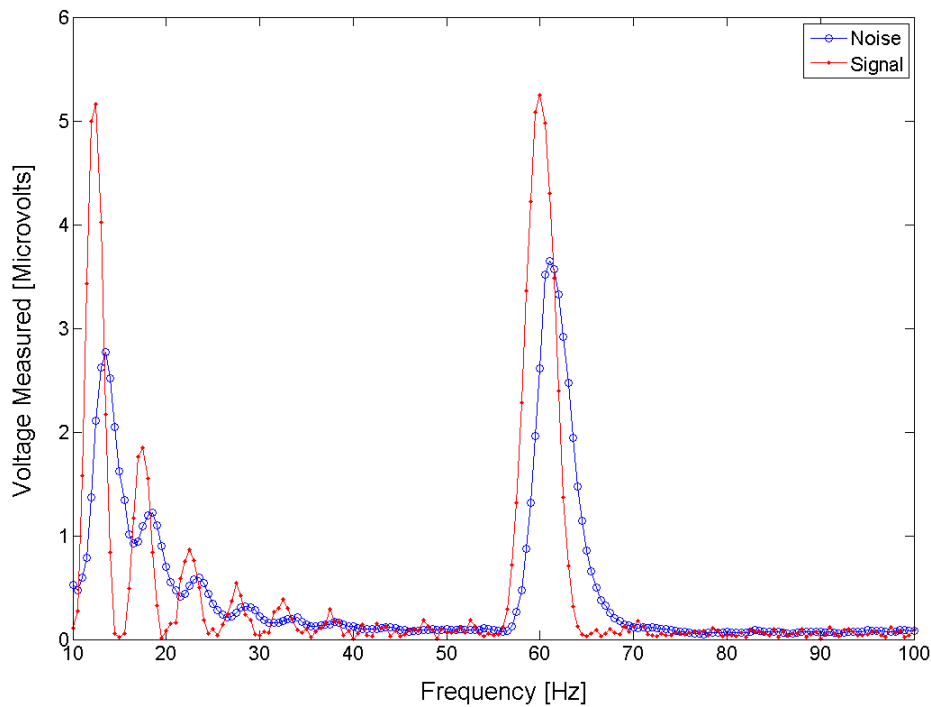


Figure 8: Voltage amplitude at the reference frequency (This will be the signal when the sample is present) and noise as a function of frequency when the lock-in amplifier is disconnected from the coils.

From the measured signal and noise we notice that there is a spike in the plot at around 60 Hz. This happens to be the utility frequency in the United States, or the frequency of the oscillations of alternating current transmitted through the power lines to the user. At this frequency we will have excessive external sources of signal, so we should avoid using frequencies around 60 Hz. The other fluctuations look like an interference pattern.

Next, we hooked the coils to the lock-in amplifier and measured the signal and noise as a function of the frequency at a constant amplitude of 0.05 Volts with no sample attached to the rod and the external magnet was turned off. We obtained the results shown in Figure 9.

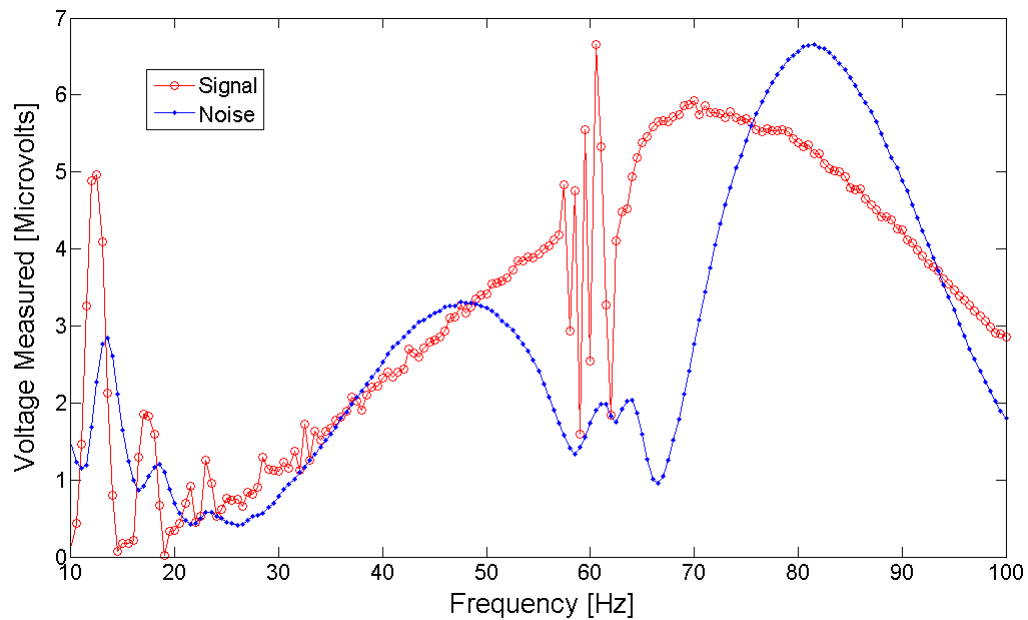


Figure 9: Noise as a function of frequency when no sample is attached and the external magnet is off. The amplitude is constant at 0.05 volts.

The magnitude is similar to the measurements with the coils not connected to the lock-in amplifier, but there is a gradual increase in signal as frequency increases. The noise also increases as the frequency increases from around 30-50 Hz and 70-85 Hz, which were low-noise regions in Figure 8.

Next we turn on the external magnetic field to see how it affects the noise. We measure once with the magnetic field set to 1000 Oe and then once with the magnetic field set to 0 Oe, but the magnet power supply still on. The following graph displays these results superimposed on the previous results.

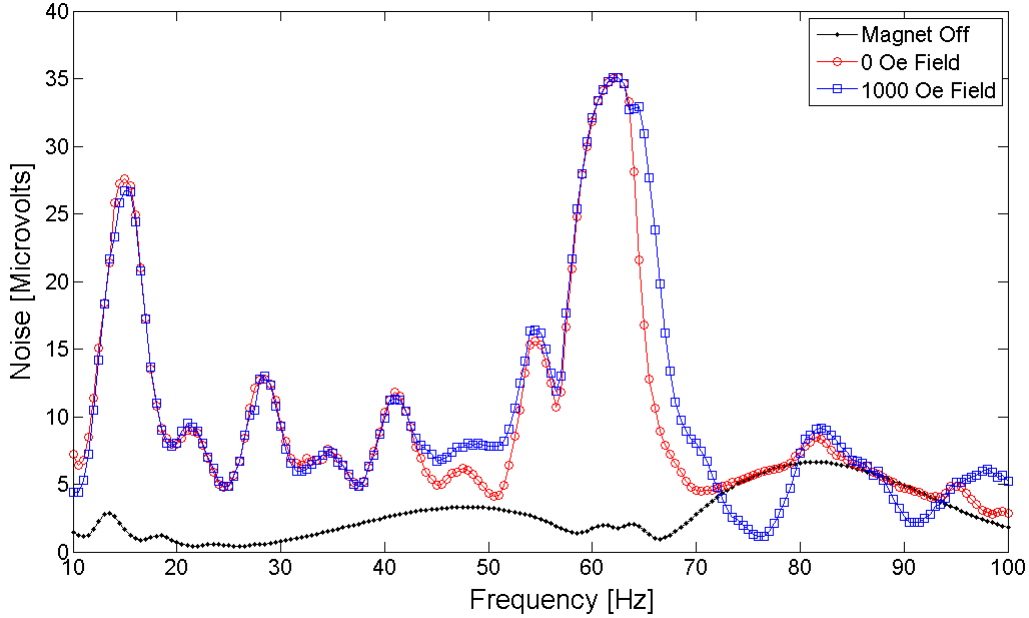


Figure 10: Plots of the noise when the magnet is set to 1000 Oe, 0 Oe, and when the magnet is turned off.

From these measurements we can draw several conclusions. First, by just turning the magnet power supply on, we pick up significantly higher noise. Even in the local minima the noise is still approximately $5 \mu\text{V}$, which is an order of magnitude higher than the noise with the magnet power supply off. Second, turning on a large field does not change the noise very much. At this point we decided that using our external electromagnets would not be a good solution for constructing a magnetometer because the signals we will be measuring will be on the order of $0.1 \mu\text{V}$.

However, with this set-up we attempted to measure the induced voltage in the coils as a function of external field with a strongly magnetic sample. I chose a piece of permalloy that weighed 0.867 g and had a volume of 0.1 cm^3 . The saturation magnetization of permalloy at room temperature is about 750 emu/cm^3 , so the magnetic moment is 75 emu , or $.075 \text{ J/T}$. Using equation (10), we estimate a signal of 2×10^{-4} Volts. For this estimate I used $\omega = 40$, $X_0 = 0.3 \text{ cm}$, $N_{turns} = 3000$, $x = 4.5 \text{ cm}$, $z =$

1.5 cm, $r = 4.74$ cm, and $A = 7$ cm².

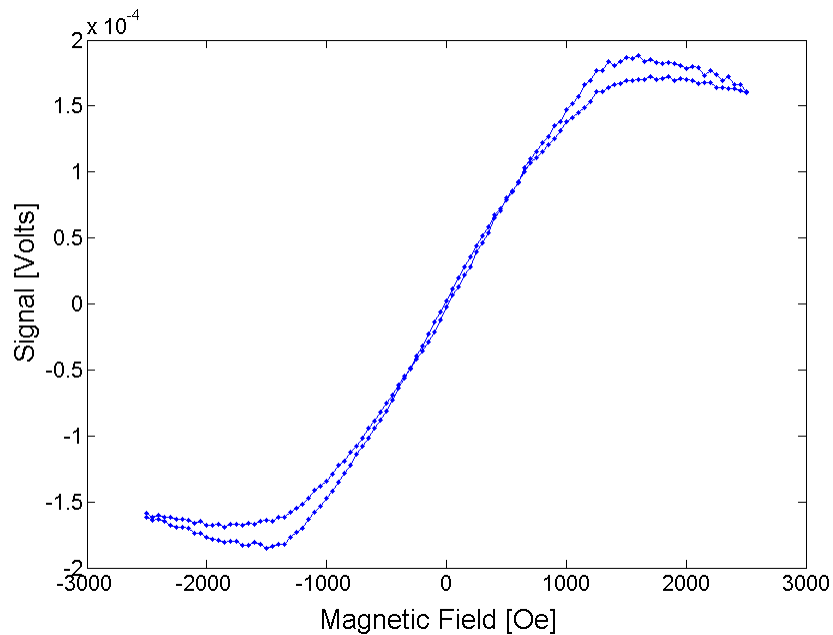


Figure 11: Here we measured the induced voltage in the coils as a function of external field.

The induced voltage measured in the coils was proportional to the external field at small fields, but near the predicted saturation magnetization level, the voltage stopped increasing as a function of the external field. At large fields, all of the magnetic poles in the metal become aligned, so that the magnetization of the sample cannot increase at the same rate and slows down. For typical permalloy magnetization curves, the magnetization still increases, but at a slower rate. This measurement at least provides evidence that our original vibrating sample magnetometer design worked. However, it is possible that the saturation we were seeing in the plot comes from the metal making the magnetic poles, so we would need to insert a hall probe during the measurements to check if the magnetic field outside of the poles is what we think it is. However, since we were planning on redesigning the VSM anyway, we instead began to work on the new design.

The last step before coming up with a new magnetometer design was to check if the noise levels we measured came from the magnet power box or actually came from the current in the electromagnet. To verify this, we left the magnet power supply on but unplugged the cable that ran from the magnet power supply box to the electromagnet. However, when we did this, the noise levels in the measurements decreased back to the low levels seen with the magnet power box off. From this we concluded that we could not use our electromagnet for the VSM.

9 New Design

We put strong permanent magnets into our setup and then measured the noise through coils as a function of frequency while the electromagnet power was off. We obtained the following curve:

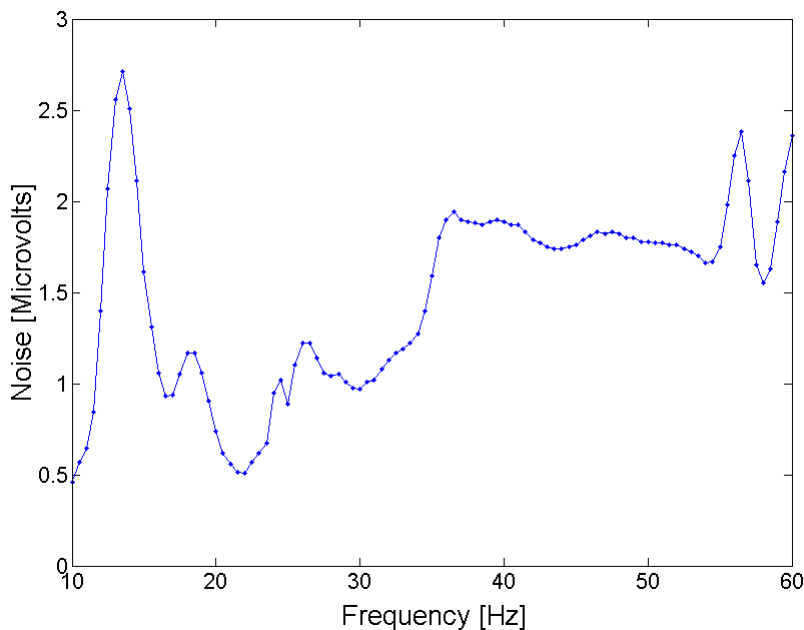


Figure 12: Noise with permanent magnets used in our setup instead of the electromagnets. Note that the scale of these measurements is much smaller.

The noise measured using permanent magnets was much smaller than the noise using the electromagnets, and it was comparable to the noise in Figure 9, so we decided we needed to redesign the VSM to incorporate permanent magnets instead. We redesigned the magnetometer so that the sample would vibrate between two permanent magnets that were moved by a very precise stepping motor. This way, we could change the external field by moving the magnets. With a calibration curve we would know the magnetic field at the sample's position as a function of how far away the magnets were from the sample.

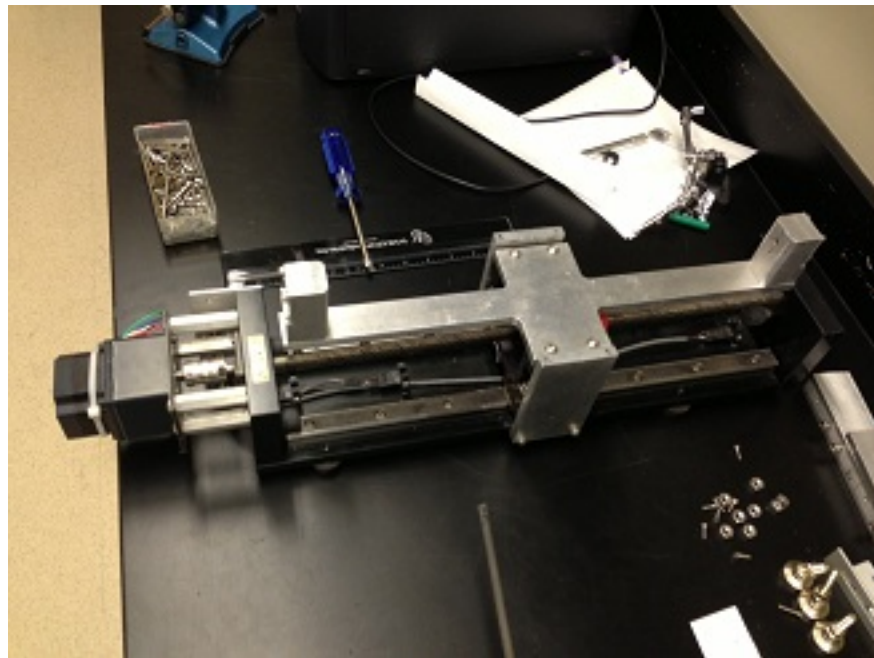


Figure 13: The setup for the magnetometer designed around the permanent magnets. The two magnets are on the left and right ends of the metal “t” in the center. The stepper motor is on the left.

The design for the new device will have the same orientation as before except that the speaker will be on the side instead of on top of the device. Theoretically we could make the speaker much closer to the magnet with this setup; however, we first needed to test how the distance between the coils and the speaker magnet affects the noise in

the coils. I measured the noise in the coils at three different distances as a function of frequency (Figure 14).

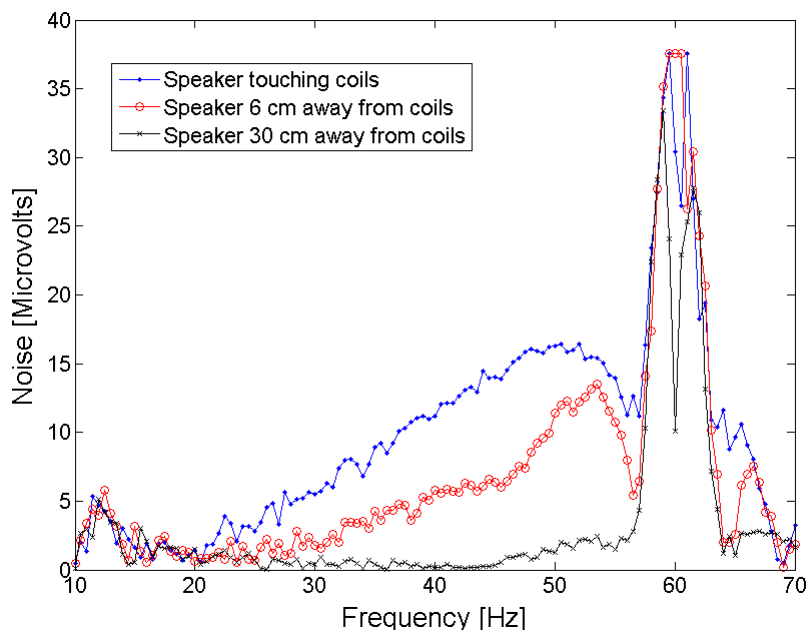


Figure 14: Noise as a function of frequency for several different distances between the pick-up coils and the base of the speaker mount. Proximity to the speaker greatly increases the noise, especially as the frequency increases.

From this data, we decided that we needed to design the VSM so that the speaker will be far from the pick-up coils. Our latest design has the coils mounted to the same apparatus to which the magnets attach, while the speaker has a separate mount on the side that holds it at the correct height. Another benefit of the new design is that we can place the coils much closer to the sample. With the new set-up, we estimate the signal of our samples to be around $1 \mu\text{V}$. This is greater than the noise measurements with the permanent magnets. At this point these parts are still being designed.

Part III

Conclusion and Future Work

The first magnetometer design showed that most of our design was effective. When the external magnet was off, the measured noise was below $1 \mu\text{V}$. When we used the large sample we were able to obtain magnetization curves as expected. We learned several ways to improve magnetometers. First, a speaker amplifier can be used, but if it is not adapted for long, uninterrupted use, it will get too hot and melt the electronics. We used a fan and a large heat sink to dissipate heat from our amplifier, after which it no longer overheated. Second, the distance between the speaker and the pick-up coils is important, because the speaker magnet will cause more noise in the measurements. Third, electromagnets are ineffective as external magnets unless they are made to have very precise fields. Permanent magnets have fields that are stable and not as noisy. The final design of the magnetometer will potentially have noise levels of $0.5\mu\text{V}$. Our estimated signal with this setup is on the order of $0.1 \mu\text{V}$, so the signal should be detectable, though the measurements will take some time unless we find more ways to increase the signal.

Future work on this project will include finishing the final design of the magnetometer and testing whether it can measure magnetization of a ferromagnet thin film. Then, we can calibrate the magnetometer by measuring the magnetizations of materials with known magnetizations. Once the device is calibrated, we can use it to measure accurately the magnetizations of thin films of alloys made from different concentrations of gadolinium and permalloy. Then, we build many samples with ferromagnetic layers of known and different magnetizations, so that we can see how the magnetization of platinum changes when it couples with ferromagnetic thin films of

different magnetizations.

References

- [1] W.L Lim, N. Ebrahim-Zadeh, H.G.E. Hentschel, and S. Urazhdin. *Appl. Phys. Lett.* (in press 2013).
- [2] D. Griffiths. *Introduction to Electrodynamics*, 3rd ed., (Prentice-Hall 1999).
- [3] C. Housecroft and A.G. Sharpe, *Inorganic Chemistry*, 3rd ed., (Prentice-Hall 2007).
- [4] E.C. Stoner, *Proceedings of the Royal Society of London A* **165**, 372 (1938).
- [5] L. Xiao and L.Wang, *J. Phys. Chem. A* **108**, 8605 (2004).
- [6] X. Liu, M. Bauer, H. Bertagnolli, E. Roduner, J. van Slageren and F. Phillipp, *Phys. Rev. Lett.* **97**, 253401 (2006).
- [7] Y. Sakamoto, Y. Oba, H. MAki, M. Suda, Y. Einaga, T. Sato, M. Mizumaki, N. Kawamura, and M. Suzuki, *Phys. Rev. B* **83**, 104420 (2011).
- [8] A. Smogunov, A. del Corso, and E. Tosatti, *Phys. Rev. B* **78**, 014423 (2008).
- [9] A. Delin and E. Tosatti, *Phys. Rev. B* **68**, 144434 (2003); *Surface Science* 262-267, 566 (2004).
- [10] X. Teng, W.-Q. Han, W. Ku, and M. Hucker *Angew. Chem. Int. Ed.* **47**, 2055 (2008).
- [11] A.M.N. Niklasson, S. Mirbt, H.L. Skriver, and B. Johansson, *Phys. Rev. B* **56**, 3276 (1997).

- [12] P. Thapa, P. Kharel, R. Sabirianov, M. Faiz, J. Borchers, D. Sellmyer, and B. Nadgorny, American Physics Society meeting, abstract No. J13.009 (2012).
- [13] S. Foner, *Rev. Sci. Instr.* **30**, 548 (1959).
- [14] W.P. Wolf, *J. Appl. Phys.* **28**, 780 (1957).
- [15] A. Niazi, P. Poddar, and A.K. Rastogi, *Current Science*, **Vol. 79, NO. 1**, 99-109 (2000).
- [16] D.O. Smith, *Rev. Sci. Instr.* **27**, 261-269 (1956).
- [17] P.A. Temple, *Am. J. Phys.* **43**, 801 (1975).
- [18] L.F. Bates. *Modern Magnetism*, (Cambridge Universtiy Press 1951)
- [19] S. Foner, *Rev. Sci. Instr.* **27**, 548-557 (1956)
- [20] S. Kundu and T.K. Nath. (Archive)
- [21] R.V. Krishnan and A. Banerjee, *Rev. Sci. Instr.* **70**, 85-92 (1997).
- [22] A. Zieba and S. Foner, *Rev. Sci. Instr.* **53**, 1344-1355 (1982).
- [23] J. Mallinson. *J. Appl. Phys.* **37**, 2514-2515 (1966).
- [24] R. Gupta, M. Gupta, and T. Gutberlet, *Pramana - J. Phys.* **71**, 1123-1127 (2008).
- [25] S.R. Hoon, *Eur. J. Phys.* **4**, 61-67 (1983).P.A. Temple, *Am. J. Phys.* **43**, 801 (1975).
- [26] B.C. Dodrill, *The Performance of the Model 7400 VSM: Sensitivity*, Lake Shore Cryotronics (2009).

- [27] M.A. Ruderman and C. Kittel, *Phys. Rev.* **96**, **99** (1954); T. Kasuya, *Prog. Theor. Phys.* **16**, **45** (1956); K. Yosida, *Phys. Rev.* **106**, 893 (1957).
- [28] J.C. Slonczewski, *J. Magn. Magn. Mater.* **150**, 13 (1995).
- [29] M.N. Baibich , J.M. Broto, A. Fert, F. Nguyen Van Dau, F. Petroff, P. Eitenne, G. Creuzet, A. Friederich, and J. Chazelas, *Phys. Rev. Lett.* **61**, 2472 (1988).
- [30] R.H. Liu, W.L Lim, S. Urazhdin, arXiv:1210.2758.
- [31] H.D. Arnold and G. W. Elmen, *Bell System Tech. J.* **2**, 101-111 (July 1923).